



First Observations of the Disruption of the Earth's Foreshock Wave Field During Magnetic Clouds

L. Turc, O. Roberts, M. Archer, M. Palmroth, M. Battarbee, T. Brito, U.
Ganse, M. Grandin, Y. Pfau-kempf, C. Escoubet, et al.

► To cite this version:

L. Turc, O. Roberts, M. Archer, M. Palmroth, M. Battarbee, et al.. First Observations of the Disruption of the Earth's Foreshock Wave Field During Magnetic Clouds. Geophysical Research Letters, American Geophysical Union, In press, 10.1029/2019GL084437 . hal-02408174

HAL Id: hal-02408174

<https://hal.archives-ouvertes.fr/hal-02408174>

Submitted on 12 Dec 2019

HAL is a multi-disciplinary open access archive for the deposit and dissemination of scientific research documents, whether they are published or not. The documents may come from teaching and research institutions in France or abroad, or from public or private research centers.

L'archive ouverte pluridisciplinaire **HAL**, est destinée au dépôt et à la diffusion de documents scientifiques de niveau recherche, publiés ou non, émanant des établissements d'enseignement et de recherche français ou étrangers, des laboratoires publics ou privés.

First observations of the disruption of the Earth's foreshock wave field during magnetic clouds

L. Turc¹, O. W. Roberts^{2,3}, M. O. Archer⁴, M. Palmroth^{1,5}, M. Battarbee¹, T.
Brito¹, U. Ganse¹, M. Grandin¹, Y. Pfau-Kempf¹, C. P. Escoubet³, and I.
Dandouras⁶

¹Department of Physics, P.O. Box 68, 00014 University of Helsinki, Finland

²Space Research Institute, Austrian Academy of Sciences, Schmiedlstrasse 6, 8042 Graz, Austria

³Directorate of Science, European Space Research and Technology Centre (ESA/ESTEC), Keplerlaan 1,
2201 AZ Noordwijk, The Netherlands

⁴School of Physics and Astronomy, Queen Mary University of London, Mile End Road, London E1 4NS,
United Kingdom

⁵Finnish Meteorological Institute, P.O. BOX 503, 00101 Helsinki, Finland

⁶IRAP, Université de Toulouse / CNRS / UPS / CNES, 9 Ave. du Colonel Roche, 31400 Toulouse,
France

Key Points:

- When reaching geospace, magnetic clouds modify significantly the properties of the first geophysical region they encounter, the foreshock
- Typical foreshock quasi-monochromatic waves are replaced by a superposition of waves at different periods **with a shorter transverse extent**
- **Multiple field-aligned beams observed during one event suggest a link between the multiple wave periods and the suprathermal ion properties**

Corresponding author: Lucile Turc, lucile.turc@helsinki.fi

Abstract

The foreshock, extending upstream of Earth’s bow shock, is a region of intense electromagnetic wave activity and nonlinear phenomena which can have global effects on geospace. It is also the first geophysical region encountered by solar wind disturbances journeying towards Earth. Here, we present the first observations of considerable modifications of the foreshock wave field during extreme events of solar origin called magnetic clouds. **Cluster’s multi-spacecraft data reveal that the typical quasi-monochromatic foreshock waves can be completely replaced by a superposition of waves with a shorter correlation length. Global numerical simulations further confirm that the foreshock wave field is more intricate and organized at smaller scales.** Ion measurements suggest that changes in shock-reflected particle properties may cause these modifications of the wave field. This state of the foreshock is encountered only during extreme events at Earth, but **intense magnetic fields are typical close to the Sun or other stars.**

Plain Language Summary

Solar storms are giant clouds of particles ejected from the Sun into space during solar eruptions. When solar storms are directed towards Earth, they can cause large disturbances in near-Earth space, for example disrupting communications or damaging spacecraft electronics. Understanding in detail what happens when solar storms reach Earth is crucial to mitigate their effects. Using measurements from the Cluster spacecraft, we investigate how solar storms modify the properties of the very first region of near-Earth space they encounter when journeying towards Earth. This region, called the foreshock, extends ahead of the protective bubble formed by the Earth’s magnetic field. The foreshock is home to intense electromagnetic waves, and disturbances in this region can perturb the Earth’s magnetic bubble. Our study reveals that solar storms modify profoundly the foreshock, resulting in a more complex wave activity. Global numerical simulations performed with the Vlasiator code confirm our findings. These changes could affect the regions of space closer to Earth, for example in modifying the wave properties or the amount of solar particles entering the Earth’s magnetic **bubble**. This needs to be taken into account to better anticipate the effects of solar storms at Earth.

1 Introduction

Magnetic clouds are strongly geoeffective solar transients, causing the most intense geomagnetic storms (Huttunen et al., 2005; Yermolaev et al., 2012). They are characterized by an enhanced magnetic field (compared to that of the regular solar wind), which rotates smoothly for multiple hours as the magnetic cloud passes by Earth. Considerable efforts have been put into determining coupling functions between the magnetic clouds’ parameters and their effects in geospace, but no one-to-one correspondence has been achieved so far, demonstrating that a more thorough understanding of the interaction of magnetic clouds with near-Earth space is still needed.

Located sunward of the bow shock, the foreshock is the first region that incoming magnetic clouds encounter when journeying towards Earth. The foreshock is permeated with intense electromagnetic waves, generated through instabilities due to the interaction of shock-reflected particles with the solar wind (Eastwood, Lucek, et al., 2005; Wilson, 2016). It extends upstream of the quasi-parallel sector of the Earth’s bow shock, where the θ_{Bn} angle between the interplanetary magnetic field (IMF) and the bow shock normal is below $\sim 45^\circ$ (Eastwood, Lucek, et al., 2005). Foreshock processes can have global effects on the Earth’s magnetosphere, causing enhanced wave activity in the downstream magnetosheath (Dimmock et al., 2016) and down to the Earth’s surface (Bier et al., 2014), or triggering fast magnetosheath jets, which can cause impulsive penetration of plasma into the magnetosphere and trigger magnetic reconnection (Plaschke et al.,

2018). Changes in the foreshock properties can therefore significantly affect conditions throughout geospace.

The most common waves in the Earth’s ion foreshock are the so-called 30 s waves (Eastwood et al., 2002). They appear as quasi-monochromatic magnetic field fluctuations at a period around 30 s with a left-hand polarization in the spacecraft frame. **Their wavelength is about 1 R_E (1 Earth radius = 6371 km), while their transverse extent is finite and ranges between 8 and 18 R_E (Archer et al., 2005). Close to the wave vector, the wave front is essentially planar over several R_E , and the overall shape of the waves is that of an oblate spheroid (Archer et al., 2005).** They have been identified as fast magnetosonic waves propagating sunward in the plasma frame, but advected earthward by the faster solar wind flow (Eastwood, Balogh, et al., 2005a). They are excited by backstreaming field-aligned beams (FABs) via the right-hand resonant ion-ion beam instability. **The cyclotron resonance condition associated with this mode is:**

$$\omega = V_{\text{beam}} k_{\parallel} - \Omega_{\text{ci}} \quad (1)$$

where V_{beam} is the beam velocity and Ω_{ci} is the ion gyrofrequency (e.g., Eastwood, Balogh, et al. (2005a)).

It is noteworthy that in spacecraft measurements, these waves are not observed in conjunction with the FABs that generated them, but with intermediate, gyrating or gyrophase-bunched ion distributions, which are thought to have evolved from the FABs (Eastwood, Balogh, et al., 2005a; Kempf et al., 2015). Measurements taken shortly before or after the spacecraft enters or exits the foreshock wave field have brought quantitative evidence of a cyclotron resonance between the FABs and the waves, lending further support to the FABs being the source of the waves (Eastwood, Lucek, et al., 2005, and references therein). These waves have been extensively studied since their discovery (Greenstadt et al., 1968; Eastwood, Balogh, et al., 2005a, 2005b; Palmroth et al., 2015), and it is well-established that their period depends on the IMF strength and orientation (Takahashi et al., 1984; Le & Russell, 1996).

Even though magnetic clouds are the most geoeffective solar wind disturbances in light of space weather events, there are no studies focusing on the foreshock properties during passing magnetic clouds. Recent numerical simulations predict that an increase in the IMF strength, as is encountered during magnetic clouds, could strongly affect the properties and the large-scale structuring of the foreshock waves (Turc et al., 2018). These simulations were however limited to a single set of solar wind conditions, warranting a more general observational investigation.

2 Event identification

Observations of foreshock waves during magnetic clouds are rare, as these transients pass by Earth only about 2% of the time (Yermolaev et al., 2012), and Earth-orbiting spacecraft cross the foreshock only sporadically. We concentrate on the early phase (2001-2005) of the Cluster mission (Escoubet et al., 2001), when the spacecraft separations are similar to the wave characteristic sizes (a few hundred kilometers), which allow us to determine accurately the wave properties. Using the catalogue introduced in Turc et al. (2016), we identify events when Cluster is located in the foreshock wave field during a magnetic cloud and divide them into 5-min intervals.

Foreshock fast magnetosonic waves are mostly transverse and generally propagate at a small angle relative to the magnetic field vector (Eastwood, Balogh, et al., 2005b). Magnetic field measurements from the fluxgate magnetometer onboard Cluster (Balogh et al., 1997) are projected onto a frame where one axis is parallel to the mean magnetic field during the 5-min interval and the two others are perpendicular to it, forming a right-handed triplet. Then we perform a wavelet transform on the perpendicular magnetic field

components and calculate the wavelet phase difference, to check the wave polarization (Torrence & Compo, 1998). Intervals of steepened waves and discrete wave packets are visually identified and rejected.

In total, we find six magnetic clouds including observations of foreshock waves with polarizations consistent with magnetosonic waves, i.e., left-handed in the spacecraft frame (see Table S1 in the supporting information). These observations take place several hours after the interplanetary shock preceding the cloud has passed by Earth, and are therefore not connected to the shock-shock interaction taking place at the cloud's arrival. When their field lines are magnetically connected to the bow shock, magnetic clouds provide new upstream conditions for the foreshock to develop. These strongly differ from typical solar wind conditions, in particular due to the clouds' large IMF strength.

3 Results

3.1 A more intricate form of wave activity

During most magnetic clouds, we find that the foreshock wave field departs significantly from its usual state. To facilitate the comparison, Figure 1 shows an example of typical fast magnetosonic foreshock waves during quiet solar wind conditions on 18 February 2003 analyzed in previous studies (Archer et al., 2005; Kis et al., 2007; Hobara et al., 2007) (left) together with representative observations during a magnetic cloud event on 19 January 2005 (right). In both cases, foreshock waves appear as large-amplitude magnetic field oscillations, especially in the two perpendicular components (panels c-d and i-j). During quiet conditions, the wavelet power spectrum showcases a rather narrow band of strong wave power around 30 s (panel e), while during magnetic clouds (panel k) high fluctuation power is observed at periods between 5 and 30 s. The magenta contours highlight where the wave power is strongest, and show that the fluctuations are left-handed in the spacecraft frame (in blue in the phase difference plot, panel l).

Cluster's measurements prior to the observations of the foreshock waves allow us to determine which parts of the foreshock the spacecraft is probing. Before 13:34 UT on 19 January 2005, Cluster was located just outside the Earth's foreshock. The rotation of the IMF inside the magnetic cloud results in a progressive change of the θ_{Bn} angle along the field line connecting Cluster to the bow shock from 60° at 13:30 UT to 40° at 14:00 UT, according to a model bow shock (Jeřáb et al., 2005). Consequently, the spacecraft probe the outer part of the foreshock, populated by FABs, from 13:34 UT, and then the foreshock wave field from 13:42 UT. In such a configuration, one would expect to observe the usual quasi-monochromatic fast magnetosonic waves. However, the power spectra of the left-handed foreshock waves display multiple spectral peaks whose periods vary with time (Figure 1k). This intricate spectrum is neither associated with right-handed polarization (in red in the phase difference plot), nor with highly steepened waves.

To identify the wave mode, we apply two independent methods, multi-spacecraft timing analysis (Schwartz, 1998) (applied to bandpass filtered data to separate the different wave periods) and multipoint signal resonator (MSR) (Narita et al., 2011), to this interval (see supporting information). Their results for the first minutes of the data set are given in Table S2 in the supporting information. The timing analysis yields wave vectors within 30° of the magnetic field. With the MSR technique, we find that the power distribution in wave vector space maximizes at two different wave vectors, showing the coexistence of two waves. The orientation of all wave vectors \mathbf{k} towards $-x$ (i.e. earthward) and the negative wave velocities in the plasma frame $V_{\text{wave,pl}}$ indicate that the waves propagate sunward in the plasma frame and are intrinsically right-handed. This rules

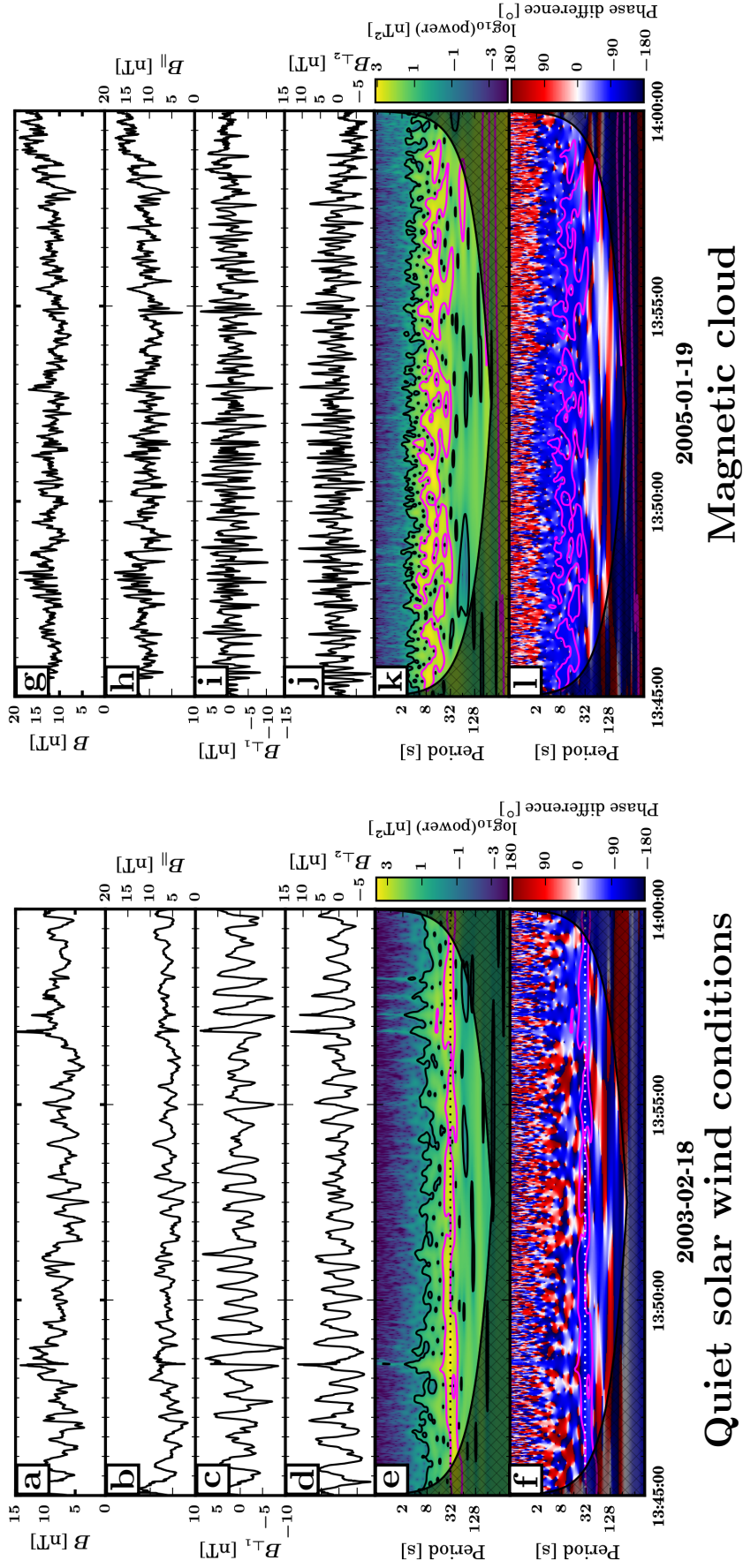


Figure 1. Foreshock waves on 18 February 2003 (left), during quiet solar wind conditions, and on 19 January 2005 (right), during a magnetic cloud. From top to bottom: magnetic field strength and components parallel and perpendicular to the mean magnetic field vector, wavelet power spectrum of $B_{\perp 1}$ and wavelet phase difference between $B_{\perp 1}$ and $B_{\perp 2}$. The dotted lines in panels e-f show the 30 s period. The black contour in panels e and k delineate the 95% confidence level. The hatched areas in panels e-f and k-l show the cone of influence, where edge effects become significant in the wavelet spectrum. The pink contour is drawn at 70% of the maximum wave power in the interval, in order to highlight the area of high wave power.

out the possibility that these are 10 s Alfvén waves, intrinsically left-handed (Eastwood et al., 2003). The Alfvén velocity was about 294 ± 158 km/s during this interval, the large uncertainties being due to large density fluctuations, as measured by the Cluster Ion Spectrometer (CIS) (Rème et al., 2001). The estimated wave speeds are comparable to the Alfvén velocity, which is close to the fast magnetosonic speed when the IMF strength is large. These properties are all consistent with that of fast magnetosonic waves.

Both wave analysis techniques therefore consistently identify a superposition of fast magnetosonic waves at different periods, ranging between 6 and 17 s. These periods, lower than the usual 30 s, are due to the magnetic cloud’s large IMF strength, here 11 nT, while its average value at Earth is about 5 nT. **The frequency of foreshock fast magnetosonic waves changes with the IMF strength because their dispersion relation depends on this parameter, among others (?, ?).** According to the Takahashi et al. (1984) empirical formula, the wave period should be 17 s under these solar wind conditions, very similar to the 18 s predicted by the Le and Russell (1996) formula, and consistent with the largest periods we observe. However, the lower wave periods are not accounted for by these models.

Highly variable wavelet spectra similar to that shown here are observed during four out of the six magnetic clouds under study here (see the third column of Table S1). The waves were identified as fast magnetosonic waves during three of these events (22 January 2004, 19 January 2005 and 22 January 2005). For the 15 May 2005 magnetic cloud, the wave mode could not be determined because of the extremely large IMF strength and solar wind velocity, resulting in the spacecraft tetrahedron being too large compared to the wavelength, thus making it impossible to identify uniquely the wave fronts.

The remaining two events display smoother wavelet spectra, resembling those observed during normal solar wind conditions. The nature of the waves could not be confirmed during the 28 March 2001 event because of the poor correlation between the spacecraft time series, due to one spacecraft being more than 1000 km apart from the others, and because of the large uncertainties in the flow velocity due to the very low density ($\simeq 0.2 \text{ cm}^{-3}$). Both events with smoother spectra were associated with much larger IMF cone angles (about 45°) than the more complex spectra (less than 30°), where the cone angle is measured between the IMF vector and the Sun-Earth line. Larger cone angles result in larger wave periods for a given IMF strength (Takahashi et al., 1984; Le & Russell, 1996), about 30 s on 23 April 2001. This suggests that the development of more complex wave activity in the foreshock is linked with shorter absolute wave periods.

3.2 A possible source for multiple fast magnetosonic waves

The superposition of fast magnetosonic waves in the foreshock associated with higher IMF strength has also been reported in a recent numerical study (Turc et al., 2018). In the simulation, the multiple wave periods were attributed to ion velocity distribution functions (VDFs) with multiple FABs, instead of the single beam which usually generates quasi-monochromatic waves.

During all intervals under study, the ion VDFs have already evolved into intermediate and gyrating ion distributions when foreshock waves are observed, in agreement with previous works (e.g., Eastwood, Balogh, et al. (2005a)). Cluster however probed the FAB beam region shortly before most of these intervals. We focus here only on those intervals for which fast magnetosonic waves were reliably identified (23 April 2001, 22 January 2004, 19 January 2005 and 22 January 2005). First we checked that the solar wind conditions remained essentially steady from Cluster’s observations of the FABs to that of the foreshock waves, with the exception of the IMF direction, which causes the foreshock wave field to reach the spacecraft. Therefore, we can reasonably assume that the FABs we observe in the first place are representative of those generating the waves detected a few minutes later.

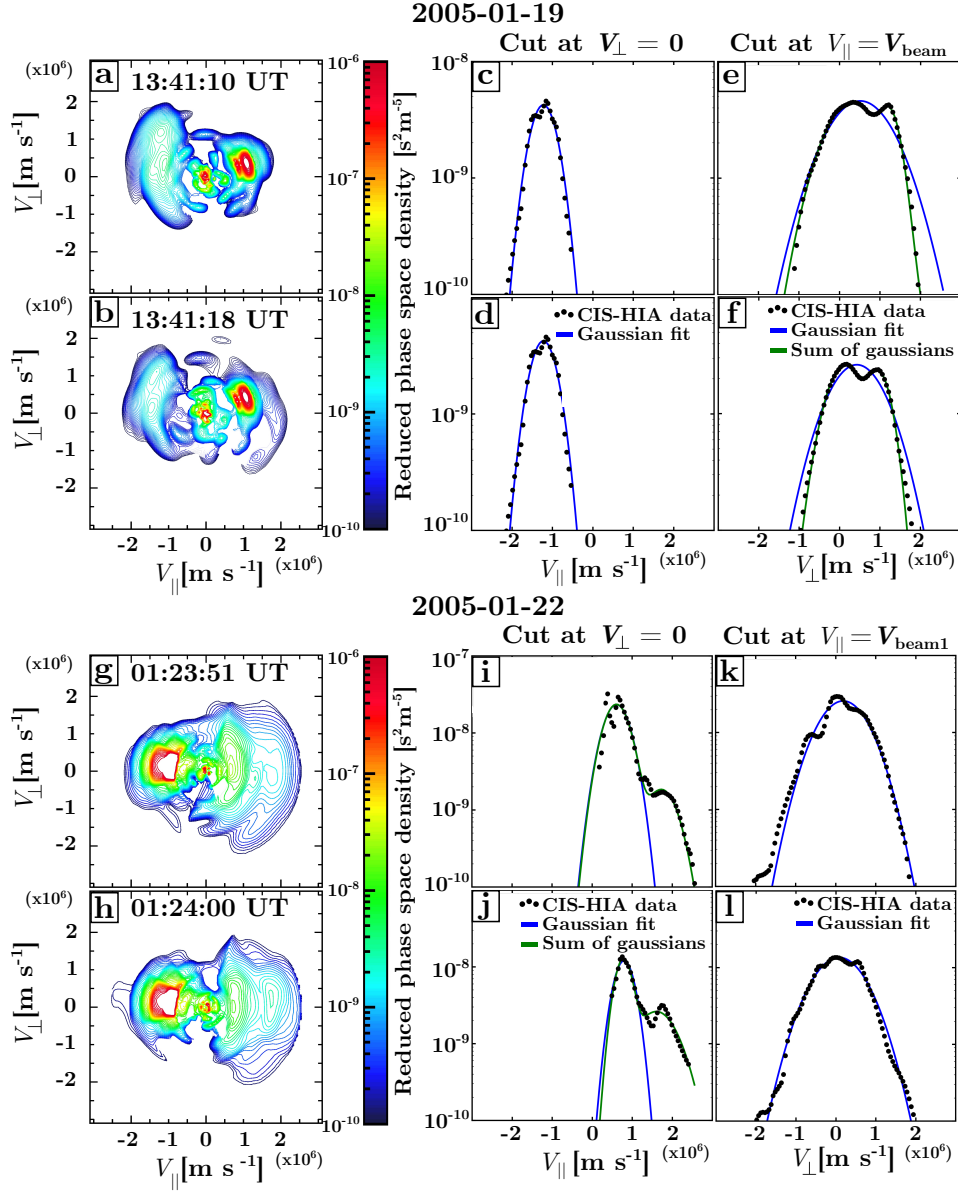


Figure 2. Ion VDFs observed shortly before the foreshock waves. Upper part: 19 January 2005 event. Lower part: 22 January 2005 event. Left column: reduced 2D VDFs, integrated over the second perpendicular velocity direction. Color-coded is the phase space density. The x- and y-axis are along and perpendicular to the direction of the magnetic field, respectively. Middle and right columns: cuts through the reduced distribution functions shown in the left column, at $V_{\perp} = 0$ (middle) and $V_{\parallel} = V_{\text{beam}}$ (right).

The upper part of Figure 2 displays representative VDFs recorded by the Hot Ion Analyzer (HIA) instrument onboard Cluster-1 at 13:41:10 and 13:41:18 UT on 19 January 2005. The left column shows reduced two-dimensional (2D) VDFs in the $(V_{\parallel}, V_{\perp})$ plane (relative to the magnetic field vector), integrated over the second perpendicular direction. In panels a and b, the solar wind population appears in red in the right-hand side, while backstreaming ions are in the left-hand side. The suprathermal population consists mostly of a FAB, centered at $V_{\parallel} \sim -1500 \text{ km s}^{-1}$. There is no clear evidence of multiple distinct FABs during this event, but a second population is observed at a non-zero pitch angle, centered around $V_{\perp} \simeq 1000 \text{ km s}^{-1}$. Panels c-d show the phase space density of the suprathermal population along a cut at $V_{\perp} = 0$. The beam shape is well fitted by a Gaussian (see also Table S3 in the supporting information), most likely because the gyrating population is located at about the same V_{\parallel} as the FAB. This second population appears as a second peak in phase space density on the cuts along V_{\perp} at $V_{\parallel} = V_{\text{beam}}$ (panels e-f), **and remain clearly visible for a range of V_{\parallel} (not shown)**. The suprathermal population is better fitted by a sum of two Gaussians in these cuts (see Table S3), **thus confirming that the two peaks are well distinct**.

During the 23 April 2001 event, typical quasi-monochromatic foreshock waves were observed, accompanied with typical FABs. During the 22 January 2004 event, a sharp rotation of the IMF shortly before 12:00 UT causes a rapid motion of the foreshock boundary past Cluster's position. Only 2 to 3 VDFs are recorded when Cluster crosses the FAB region, and given the rapid motion of the boundary, it is difficult to draw firm conclusions regarding the characteristics of the FABs during this event.

Finally, the 22 January 2005 event brings clear evidence of multiple FABs similar to those observed in numerical simulations (Turc et al., 2018), displayed in the bottom part of Figure 2. Note that because of the different IMF orientation, the solar wind core in panels g and h is at negative parallel velocities during this event. The beams are centered around $V_{\parallel} \sim 700 \text{ km s}^{-1}$ and 1700 km s^{-1} , respectively, and are well fitted by a sum of two Gaussians (panels i-j and Table S3). From these fits and Gaussian fits along V_{\perp} at $V_{\parallel} = V_{\text{beam1}}$ (panels k-l) and $V_{\parallel} = V_{\text{beam2}}$, we estimate the temperature anisotropy (ratio of the perpendicular to parallel temperatures) of each of the beams (see Table S4). They range between 2 and 10, in excellent agreement with previous observations (Paschmann et al., 1981). The two FABs evolve progressively from one measured distribution function to the next for about a minute. At 01:24:00 UT, the higher energy beam reaches its highest phase space density, peaking at about $1.3 \text{ s}^2 \text{ m}^{-5}$, only a factor of three lower than the peak of the other beam, at about $4.1 \text{ s}^2 \text{ m}^{-5}$.

To our knowledge, this is the first time that multiple FABs are observed in conjunction with unusual foreshock wave activity. Spacecraft observations of multiple FABs in the foreshock have been reported previously (Meziane et al., 2011), but were associated with typical quasi-monochromatic 30 s waves. The IMF strength was relatively high (9 nT) during the main interval analyzed in Meziane et al. (2011), but was not associated with a magnetic cloud. The comparison of the cyclotron resonant speed of the waves with that of the FABs revealed that only the main beam was in cyclotron resonance with the waves (Meziane et al., 2011).

The cyclotron resonant speed of the waves, normalized to the solar wind speed, is calculated as:

$$P_{\text{res}} = \frac{\Omega_{\text{ci}} \cos \theta_{kV}}{\omega_{\text{sc}} \cos \theta_{kB}} \quad (2)$$

where ω_{sc} is the wave frequency in the spacecraft frame, and θ_{kV} (θ_{kB}) is the angle between the wave vector and the solar wind velocity vector (the IMF vector) (Meziane et al., 2011). We calculate P_{res} for the multiple FABs observed around 01:24 UT on 22 January 2005, to check whether they are in cyclotron resonance with the waves observed from 01:32 UT onwards. We find that the velocity of the lower energy beam normalized with the solar wind

speed ranges between 1.8 and 1.9, and that of the higher energy beam between 3.0 and 3.1. This is in excellent agreement with the cyclotron resonant speeds of the waves, which are 1.9 and 3.3 for the two main wave periods determined just after the onset of the waves, thus bringing strong support to the multiple FABs being the source of the waves.

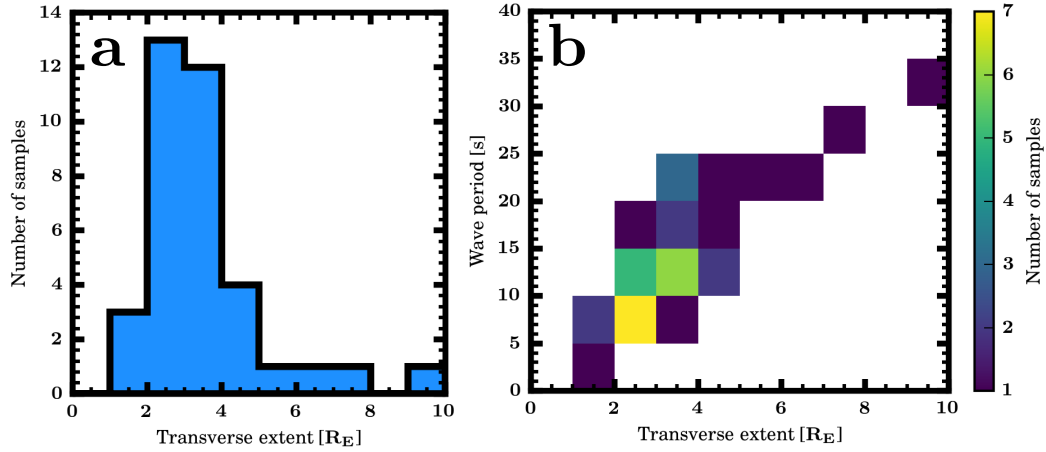
3.3 Structuring of the foreshock at smaller scales

During magnetic clouds, the period of fast magnetosonic waves is shorter, which, **in the plasma rest frame**, translates into a shorter wavelength. Another critical parameter for the structuring of the foreshock wave field is the transverse extent of the **waves**. The size of the wave fronts can be estimated using a multi-spacecraft analysis technique based on cross-correlations of measurements from pairs of spacecraft (see Archer et al. (2005) and supporting information). Here, we are interested in the wave correlation length in the **plane** perpendicular to the wave vector. We divide all our intervals of fast magnetosonic waves into 120-s sections, so that for each interval the wave period and the upstream parameters remain roughly constant while retaining a sufficient number of wave periods. We obtain a reliable estimate of the transverse extent of the wave fronts for 35 intervals, displayed as a histogram in Figure 3a. The transverse extent ranges between 1 and 10 R_E (average 3.5 R_E ; **median 3.2 R_E**). This is significantly shorter than during quiet solar wind conditions (8-18 R_E) (Archer et al., 2005). Moreover, we find that the transverse extent of the wave fronts is correlated with the wave period, as evidenced by Figure 3b. This implies that the waves retain the same aspect ratio when their wavelength varies, i.e., the ratio of their wavelength over their transverse extent is roughly constant **in the events under study**.

To get a clearer view of what these different transverse extents imply on global scales, we examine the foreshock wave field in two global simulations performed with the hybrid-Vlasov Vlasator code (von Alfthan et al., 2014; Palmroth et al., 2018), already studied in Turc et al. (2018). In both runs, the simulation domain is two-dimensional (2D) in real space and describes the equatorial plane of near-Earth space. The IMF has a 5° cone angle, the solar wind velocity is $\mathbf{V}_{SW} = (-600, 0, 0) \text{ km s}^{-1}$ and the ion density $n_{SW} = 3.3 \text{ cm}^{-3}$. The only difference between the two runs is the IMF strength, set to 5 nT in Run 1, and 10 nT in Run 2. The former corresponds to regular IMF strength at Earth, similar to that in the event studied by Archer et al. (2005), while the latter is comparable to the 19 January 2005 event (Figure 1, right).

The out-of-plane (B_z) component of the magnetic field in the simulation domain is displayed in panels c (Run 1) and d (Run 2) of Figure 3. For clarity, the regions downstream of the bow shock are not shown. Because the foreshock waves are mostly transverse, B_z is a good marker of the foreshock wave field. As can readily be seen from these plots, the wave fronts are coherent over much larger scales during quiet solar wind conditions (panel c). The plus signs indicate the barycentric positions of triplets of virtual spacecraft, separated by $\sim 1000 \text{ km}$ in order to mimic the Cluster constellation in 2D, where the transverse extent of the **waves** was estimated reliably. Since the simulation is 2D, only three spacecraft are needed to characterize the shape of the **waves** in the simulation plane. Time series of the magnetic field are extracted at each virtual spacecraft location. We apply the same cross-correlation technique as on Cluster data to estimate the transverse extent of the **waves**, albeit only with three spacecraft. The results of the analysis are shown as a histogram in panel e. We find that the transverse extent of the wave fronts varies significantly depending on the position in the foreshock. We obtain values ranging between 3 and 11 R_E in Run 1 and between 2 and 6 R_E in Run 2, the smallest values being encountered closer to the bow shock, especially in Run 1. The average transverse extent of the wave fronts is 7 R_E in Run 1 and 4 R_E in Run 2.

Cluster observations



Vlasator simulations

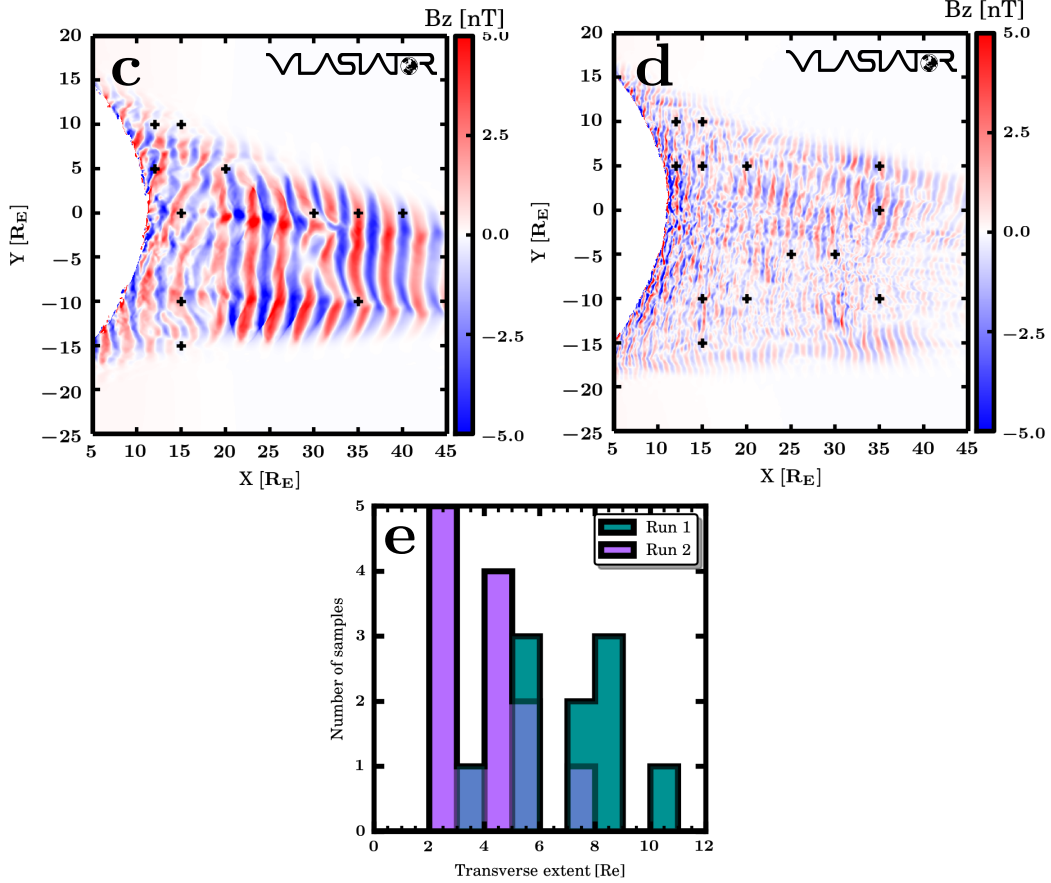


Figure 3. Transverse extent of the foreshock waves. Upper part: Cluster's observations during magnetic clouds. (a) Distribution of the transverse extent of foreshock waves. (b) Wave period as a function of the transverse extent. Bottom part: global simulations. (c) and (d) Magnetic field B_z component in Runs 1 and 2 at time $t = 500$ s from the beginning of the runs, which illustrate the foreshock wave field. The plus signs indicate the positions of triplets of virtual spacecraft where the transverse extent of the wave fronts was reliably determined. (e) Distribution of the transverse extent of the wave fronts.

These results are in reasonable agreement with Cluster data, supporting the fact that the simulated foreshock wave field is representative of the actual foreshock. This suggests that during quiet solar wind conditions, the foreshock wave field is composed of large-scale coherent wave fronts, that can extend over more than $10 R_E$ in the direction perpendicular to the wave vector. When moving closer to the bow shock, the transverse extent of the wave fronts decreases as they become more irregular. When the IMF strength is high, as is the case during magnetic clouds, the foreshock wave field breaks down into a multitude of smaller wave fronts, and thus loses its large-scale coherency.

4 Discussion and conclusions

We have presented the first observations of the Earth's foreshock during magnetic clouds, revealing that the foreshock can develop while these transients pass by near-Earth space. We found that the foreshock properties are strongly modified due to the unusual upstream conditions dictated by the clouds. Using multi-spacecraft analysis techniques, we have shown that the usually quasi-monochromatic fast magnetosonic waves are replaced by a superposition of fast magnetosonic waves at different periods. We also found that the coherence length of the waves is shorter, both along and transverse to the wave vector, suggesting that the foreshock is structured over smaller scales. Atypical ion velocity distribution functions are observed in conjunction with the unusual wave activity. During one event, we find clear evidence of two distinct FABs in cyclotron resonance with the waves observed shortly afterwards, consistent with previous numerical works (Turc et al., 2018).

In another event, we find in many instances a second suprathermal population at non-zero pitch angle together with a FAB. The gyrating population might have evolved from a second FAB, due to gyrophase trapping (Mazelle et al., 2003; Kempf et al., 2015). The lack of observations of multiple FABs during this event could also be due to the spacecraft being connected to larger θ_{Bn} values at the bow shock. Using a model bow shock, we estimate that the FABs observed by Cluster originate from $\theta_{Bn} \sim 52^\circ$ during this event, and from $\theta_{Bn} \sim 43^\circ$ when multiple FABs are observed. We also estimate that the dominant beam is associated with $\theta_{Bn} \sim 43^\circ$ in the main interval analyzed in Meziane et al. (2011). Local changes of the quasi-perpendicular shock geometry could generate multiple field-aligned beams (Meziane et al., 2011), since their energy depends on the local shock geometry upon their generation (Paschmann et al., 1980). Foreshock processes are a significant source of local shock deformations (Meziane et al., 2011). Therefore, the observations of multiple FABs being more likely at lower θ_{Bn} values, i.e., closer to the foreshock, fits well within this scenario.

We note here that the second beam in the Meziane et al. (2011) event was not associated with intricate wave activity nor with a magnetic cloud. The maximum phase space density of the second beam was about two orders of magnitude lower than that of the first beam, which could explain why it did not trigger additional fast magnetosonic waves, and thus no cyclotron resonance with the foreshock waves was found. On the contrary, on 22 January 2005, the maximum phase space densities of the two beams only differ by a factor of three, and both beams can thus generate fast magnetosonic waves of comparable amplitudes, as their growth rate increases with increasing beam density (Gary, 1991).

In this study, we have determined the wave properties assuming a linear picture, though the large amplitude of the fluctuations compared to the background field and the waveforms reminiscent of wave packets suggest that the waves have entered the nonlinear regime. Linear methods remain appropriate in this case as the spectral peaks of the waves are well-distinct, allowing to separate the different wave modes, as done previously in Hobara et al.

(2007). Nonlinear wave analysis lies beyond the scope of the present paper, but would be an interesting follow-up study.

Foreshock waves are known to modulate the shape of the shock front (Burgess, 1995). Therefore, the smaller wavelength of the fast magnetosonic waves and their smaller transverse extent could both result in smaller ripples at the shock front during magnetic clouds, which in turn can affect particle reflection at the quasi-parallel bow shock (Wu et al., 2015) and the formation of magnetosheath high-speed jets (Plaschke et al., 2018).

IMF strengths above 10 nT are relatively uncommon at Earth, as they are associated with magnetic clouds or other solar transients, but they become typical closer to the Sun. For example, at Mercury’s orbit, the average IMF strength is about 20-30 nT (Korth et al., 2011). The small size of Mercury’s magnetosphere results however in another wave mode being predominant in the foreshock, leading to a different organisation of its wave field (Le et al., 2013). Outside of our solar system, exoplanets orbiting close to their host stars are immersed in intense magnetic fields, and could thus display similar foreshock properties as presented here.

Acknowledgments

This project has received funding from the European Union’s Horizon 2020 research and innovation programme under the Marie Skłodowska-Curie grant agreement No 704681. We acknowledge the European Research Council for Starting grant 200141-QuESpace, with which Vlasiator was developed, and Consolidator grant 682068-PRESTISSIMO awarded to further develop Vlasiator and use it for scientific investigations. The work leading to these results have been carried out in the Finnish Centre of Excellence in Research of Sustainable Space (Academy of Finland grant numbers 312351 and 312390). We thank the Cluster Science Archive (CSA) (Laakso et al., 2010) and the CIS and FGM PI teams for providing Cluster data. The CSC - IT Center for Science in Finland is acknowledged for the Pilot run and the Grand Challenge award leading to the results shown here. We thank S. von Alfthan for his major contribution in the development of Vlasiator. The left panels of Figure 2 were done with the QSAS science analysis system provided by the United Kingdom Cluster Science Centre (Imperial College London and Queen Mary, University of London) supported by The Science and Technology Facilities Council (STFC).

Data from the Cluster mission is freely available on the CSA. The Vlasiator runs described here take several terabytes of disk space and are kept in storage maintained within the CSC - IT Center for Science. Data presented in this paper can be accessed by following the data policy on the Vlasiator web site.

References

- Archer, M., Horbury, T. S., Lucek, E. A., Mazelle, C., Balogh, A., & Dandouras, I. (2005, May). Size and shape of ULF waves in the terrestrial foreshock. *Journal of Geophysical Research (Space Physics)*, *110*, A05208. doi: 10.1029/2004JA010791
- Balogh, A., Dunlop, M. W., Cowley, S. W. H., Southwood, D. J., Thomlinson, J. G., Glassmeier, K. H., ... Kivelson, M. G. (1997, January). The Cluster Magnetic Field Investigation. *Space Sci. Rev.*, *79*, 65-91. doi: 10.1023/A:1004970907748
- Bier, E. A., Owusu, N., Engebretson, M. J., Posch, J. L., Lessard, M. R., & Pilipenko, V. A. (2014, March). Investigating the IMF cone angle control of Pc3-4 pulsations observed on the ground. *Journal of Geophysical Research (Space Physics)*, *119*, 1797-1813. doi: 10.1002/2013JA019637
- Burgess, D. (1995). Foreshock-shock interaction at collisionless quasi-parallel shocks. *Advances in Space Research*, *15*, 159-169. doi: 10.1016/0273-1177(94)00098-L

- Dimmock, A. P., Nykyri, K., Osmane, A., & Pulkkinen, T. I. (2016, July). Statistical mapping of ULF Pc3 velocity fluctuations in the Earth's dayside magnetosheath as a function of solar wind conditions. *Advances in Space Research*, 58, 196-207. doi: 10.1016/j.asr.2015.09.039
- Eastwood, J. P., Balogh, A., Dunlop, M. W., Horbury, T. S., & Dandouras, I. (2002, November). Cluster observations of fast magnetosonic waves in the terrestrial foreshock. *Geophysical Research Letters*, 29, 2046-2050. doi: 10.1029/2002GL015582
- Eastwood, J. P., Balogh, A., Lucek, E. A., Mazelle, C., & Dandouras, I. (2003, July). On the existence of Alfvén waves in the terrestrial foreshock. *Annales Geophysicae*, 21, 1457-1465. doi: 10.5194/angeo-21-1457-2003
- Eastwood, J. P., Balogh, A., Lucek, E. A., Mazelle, C., & Dandouras, I. (2005a). Quasi-monochromatic ulf foreshock waves as observed by the four-spacecraft cluster mission: 1. statistical properties. *Journal of Geophysical Research: Space Physics*, 110(A11), A11219. doi: 10.1029/2004JA010617
- Eastwood, J. P., Balogh, A., Lucek, E. A., Mazelle, C., & Dandouras, I. (2005b, November). Quasi-monochromatic ULF foreshock waves as observed by the four-spacecraft Cluster mission: 2. Oblique propagation. *Journal of Geophysical Research (Space Physics)*, 110(A9), A11220. doi: 10.1029/2004JA010618
- Eastwood, J. P., Lucek, E. A., Mazelle, C., Meziane, K., Narita, Y., Pickett, J., & Treumann, R. A. (2005, June). The Foreshock. *Space Science Reviews*, 118, 41-94. doi: 10.1007/s11214-005-3824-3
- Escoubet, C. P., Fehringer, M., & Goldstein, M. (2001, October). Introduction The Cluster mission. *Annales Geophysicae*, 19, 1197-1200. doi: 10.5194/angeo-19-1197-2001
- Gary, S. P. (1991, May). Electromagnetic ion/ion instabilities and their consequences in space plasmas - A review. *Space Science Reviews*, 56, 373-415. doi: 10.1007/BF00196632
- Greenstadt, E. W., Green, I. M., Inouye, G. T., Hundhausen, A. J., Bame, S. J., & Strong, I. B. (1968, January). Correlated magnetic field and plasma observations of the Earth's bow shock. *Journal of Geophysical Research*, 73, 51. doi: 10.1029/JA073i001p00051
- Hobara, Y., Walker, S. N., Balikhin, M., Pokhotelov, O. A., Dunlop, M., Nilsson, H., & Rème, H. (2007, July). Characteristics of terrestrial foreshock ULF waves: Cluster observations. *Journal of Geophysical Research (Space Physics)*, 112, A07202. doi: 10.1029/2006JA012142
- Huttunen, K. E. J., Schwenn, R., Bothmer, V., & Koskinen, H. E. J. (2005, February). Properties and geoeffectiveness of magnetic clouds in the rising, maximum and early declining phases of solar cycle 23. *Annales Geophysicae*, 23, 625-641. doi: 10.5194/angeo-23-625-2005
- Jeřáb, M., Němeček, Z., Šafránková, J., Jelínek, K., & Měrka, J. (2005, January). Improved bow shock model with dependence on the IMF strength. *Planet. Space Sci.*, 53, 85-93. doi: 10.1016/j.pss.2004.09.032
- Kempf, Y., Pokhotelov, D., Gutynska, O., Wilson III, L. B., Walsh, B. M., von Althaus, S., ... Palmroth, M. (2015, May). Ion distributions in the Earth's foreshock: Hybrid-Vlasov simulation and THEMIS observations. *Journal of Geophysical Research (Space Physics)*, 120, 3684-3701. doi: 10.1002/2014JA020519
- Kis, A., Scholer, M., Klecker, B., Kucharek, H., Lucek, E. A., & Rème, H. (2007, March). Scattering of field-aligned beam ions upstream of Earth's bow shock. *Annales Geophysicae*, 25, 785-799. doi: 10.5194/angeo-25-785-2007
- Korth, H., Anderson, B. J., Zurbuchen, T. H., Slavin, J. A., Perri, S., Boardsen, S. A., ... McNutt, R. L. (2011, December). The interplanetary magnetic field environment at Mercury's orbit. *Planetary and Space Science*, 59, 2075-2085. doi: 10.1016/j.pss.2010.10.014

- Laakso, H., Perry, C., McCaffrey, S., Herment, D., Allen, A. J., Harvey, C. C., ...
Turner, R. (2010). Cluster Active Archive: Overview. *Astrophysics and Space
Science Proceedings*, 11, 3-37. doi: {10.1007/978-90-481-3499-1_1}
- Le, G., Chi, P. J., Blanco-Cano, X., Boardsen, S., Slavin, J. A., Anderson, B. J., &
Korth, H. (2013, June). Upstream ultra-low frequency waves in Mercury's
foreshock region: MESSENGER magnetic field observations. *Journal of Geo-
physical Research (Space Physics)*, 118, 2809-2823. doi: 10.1002/jgra.50342
- Le, G., & Russell, C. T. (1996, February). Solar wind control of upstream wave fre-
quency. *J. Geophys. Res.*, 101, 2571-2576. doi: 10.1029/95JA03151
- Mazelle, C., Meziane, K., Le Quéau, D., Wilber, M., Eastwood, J. P., Rème, H.,
... Balogh, A. (2003, October). Production of gyrating ions from nonlin-
ear wave-particle interaction upstream from the Earth's bow shock: A case
study from Cluster- CIS. *Planetary and Space Science*, 51, 785-795. doi:
10.1016/j.pss.2003.05.002
- Meziane, K., Hamza, A. M., Wilber, M., Mazelle, C., & Lee, M. A. (2011, October).
Anomalous foreshock field-aligned beams observed by Cluster. *Annales Geo-
physicae*, 29, 1967-1975. doi: 10.5194/angeo-29-1967-2011
- Narita, Y., Glassmeier, K. H., & Motschmann, U. (2011, February). High-resolution
wave number spectrum using multi-point measurements in space - the Multi-
point Signal Resonator (MSR) technique. *Annales Geophysicae*, 29, 351-360.
doi: 10.5194/angeo-29-351-2011
- Palmroth, M., Archer, M., Vainio, R., Hietala, H., Pfau-Kempf, Y., Hoilijoki, S., ...
Eastwood, J. P. (2015). Ulf foreshock under radial IMF: Themis observations
and global kinetic simulation Vlasior results compared. *Journal of Geophysi-
cal Research: Space Physics*, 120(10), 8782-8798. doi: 10.1002/2015JA021526
- Palmroth, M., Ganse, U., Pfau-Kempf, Y., Battarbee, M., Turc, L., Brito, T., ...
von Alfthan, S. (2018, August). Vlasov methods in space physics and
astrophysics. *Living Reviews in Computational Astrophysics*, 4, 1. doi:
10.1007/s41115-018-0003-2
- Paschmann, G., Sckopke, N., Asbridge, J. R., Bame, S. J., & Gosling, J. T.
(1980, September). Energization of solar wind ions by reflection from the
earth's bow shock. *Journal of Geophysical Research*, 85, 4689-4694. doi:
10.1029/JA085iA09p04689
- Paschmann, G., Sckopke, N., Papamastorakis, I., Asbridge, J. R., Bame, S. J., &
Gosling, J. T. (1981, Jun). Characteristics of reflected and diffuse ions up-
stream from the earth's bow shock. *Journal of Geophysical Research*, 86,
4355-4364. doi: 10.1029/JA086iA06p04355
- Plaschke, F., Hietala, H., Archer, M., Blanco-Cano, X., Kajdič, P., Karlsson, T.,
... Sibeck, D. (2018, Aug). Jets Downstream of Collisionless Shocks. *Space
Science Reviews*, 214(5), 4-81. doi: 10.1007/s11214-018-0516-3
- Rème, H., Aoustin, C., Bosqued, J. M., Dandouras, I., Lavraud, B., Sauvaud, J. A.,
... Sonnerup, B. (2001, October). First multispacecraft ion measurements
in and near the Earth's magnetosphere with the identical Cluster ion spec-
trometry (CIS) experiment. *Annales Geophysicae*, 19, 1303-1354. doi:
10.5194/angeo-19-1303-2001
- Roberts, O. W., Li, X., & Jeska, L. (2014, December). Validation of the k-filtering
technique for a signal composed of random- phase plane waves and non-
random coherent structures. *Geoscientific Instrumentation, Methods and
Data Systems*, 3, 247-254. doi: 10.5194/gi-3-247-2014
- Schwartz, S. J. (1998, January). Shock and Discontinuity Normals, Mach Numbers,
and Related Parameters. *ISSI Scientific Reports Series*, 1, 249-270.
- Takahashi, K., McPherron, R. L., & Terasawa, T. (1984, May). Dependence of
the spectrum of Pc 3-4 pulsations on the interplanetary magnetic field. *J. Geo-
phys. Res.*, 89, 2770-2780. doi: 10.1029/JA089iA05p02770
- Torrence, C., & Compo, G. P. (1998, January). A Practical Guide to Wavelet Anal-

- ysis. *Bulletin of the American Meteorological Society*, 79, 61-78. doi: 10.1175/1520-0477(1998)079\$(\$0061:APGTWA\$)\$2.0.CO;2
- Turc, L., Escoubet, C. P., Fontaine, D., Kilpua, E. K. J., & Enestam, S. (2016, May). Cone angle control of the interaction of magnetic clouds with the Earth's bow shock. *Geophysical Research Letters*, 43, 4781-4789. doi: 10.1002/2016GL068818
- Turc, L., Ganse, U., Pfau-Kempf, Y., Hoilijoki, S., Battarbee, M., Juusola, L., ... Palmroth, M. (2018). Foreshock Properties at Typical and Enhanced Interplanetary Magnetic Field Strengths: Results From Hybrid-Vlasov Simulations. *Journal of Geophysical Research: Space Physics*, 123(0), 5476-5493. doi: 10.1029/2018JA025466
- von Alfthan, S., Pokhotelov, D., Kempf, Y., Hoilijoki, S., Honkonen, I., Sandroos, A., & Palmroth, M. (2014, December). Vlasovator: First global hybrid-Vlasov simulations of Earth's foreshock and magnetosheath. *Journal of Atmospheric and Solar-Terrestrial Physics*, 120, 24-35. doi: 10.1016/j.jastp.2014.08.012
- Wilson, L. B. (2016, Feb). Low Frequency Waves at and Upstream of Collisionless Shocks. *Washington DC American Geophysical Union Geophysical Monograph Series*, 216, 269-291. doi: 10.1002/9781119055006.ch16
- Wu, M., Hao, Y., Lu, Q., Huang, C., Guo, F., & Wang, S. (2015, July). The Role of Large Amplitude Upstream Low-frequency Waves in the Generation of Superthermal Ions at a Quasi-parallel Collisionless Shock: Cluster Observations. *Astrophysical Journal*, 808, 2. doi: 10.1088/0004-637X/808/1/2
- Yermolaev, Y. I., Nikolaeva, N. S., Lodkina, I. G., & Yermolaev, M. Y. (2012, May). Geoeffectiveness and efficiency of CIR, sheath, and ICME in generation of magnetic storms. *Journal of Geophysical Research (Space Physics)*, 117, A00L07. doi: 10.1029/2011JA017139